Applied Catalysis B: Environmental 84 (2008) 297–302

Contents lists available at ScienceDirect

Applied Catalysis B: Environmental

journal homepage: www.elsevier.com/locate/apcatb

Comparative study of the electrocatalytic oxidation and mechanism of nitrophenols at Bi-doped lead dioxide anodes

Yuan Liu, Huiling Liu *, Yan Li

Department of Environmental Science & Engineering, State Key Laboratory of Urban Water Resources and Environment (SKLUWRE), School of Municipal and Environmental Engineering Harbin Institute of Technology, Harbin 150090, China

ARTICLE INFO

Article history:
Received 15 January 2008
Received in revised form 8 March 2008
Accepted 5 April 2008
Available online 18 April 2008

Keywords:
Nitrophenols
Electrocatalytic oxidation
Bi-doped lead dioxide anodes
Mechanisms
Hammett constant

ABSTRACT

The electrocatalytic oxidation of *o*-nitrophenol (*o*-NP), *m*-nitrophenol (*m*-NP) and *p*-nitrophenol (*p*-NP) has been studied at Bi-doped lead dioxide anodes on acid medium by cyclic voltammetry and bulk electrolysis. The results of voltammetric studies indicated that these nitrophenol isomers were indirectly oxidized by •OH radical in the solutions. Within the present experimental conditions used (50 mg of nitrophenol L^{-1}, pH 4.3, 30 mA cm^{-2}, 303 K), the complete decomposition of nitrophenols (NPs) was achieved. The electrocatalytic oxidation of NPs lay in the order: *p*-NP > *m*-NP > *o*-NP. Molecular configuration including the electron character and hydrogen bonds of NPs significantly influenced the electrocatalytic oxidation of these isomers. Hydroquinone, catechol, resorcinol, benzoquinone, aminophenols, glutaconic acid and maleic acid and oxalic acid have been detected as soluble products during the electrolysis of NPs. The possible degradation pathways of these isomers were proposed. The first stage is the release of nitro group from the aromatic rings. As a consequence, hydroquinone, catechol, resorcinol and benzoquinone are formed. These organic compounds are oxidized initially to carboxylic acids (glutaconic acid, maleic acid and oxalic acid) and later to carbon dioxide and water. Simultaneously, the reduction of NPs to aminophenols takes place at the cathode.

1. Introduction

Nitrophenols (NPs) represent a class of widely synthesized chemicals particularly involved in the manufactures of pesticides, dyes and pharmaceuticals [1–5]. NPs are anthropogenic, toxic, inhibitory and bio-refractory organic compounds and are considered as hazardous substances and priority toxic pollutants by the United States Environmental Protection Agency (USEPA), and the Public Health Service in the USA [6,7]. The USEPA recommends restricting the concentration of these NPs in natural waters in the range of 1–20 ppb [8], as it takes a long time for NPs to break down in groundwater, as well as in deep soil. The degradation of NPs by biological treatment is difficult and requires long incubation time since the presence of nitro-group confers to the aromatic compound a strong chemical stability and resistance to microbial degradation [9–12]. It is of significant importance to develop new treatment technologies for the destruction and mineralization of NPs in wastewater. In recent years, several works have been focused on different technologies such as chemical [13], sonochemical [14], adsorption [15] and advanced oxidation processes (AOPs) including Fenton [16,17], electro-Fenton [18,19], photocatalytic oxidation [20,21], catalytic wet air oxidation [22,23] and electrocatalytic oxidation [24–29].

Within these techniques, electrocatalytic oxidation appears as one of the most promising technologies for the treatment of wastewater containing small amounts of aromatic compounds. The main advantages of the electrocatalytic oxidation processes include environmental compatibility, versatility, energy efficiency, safety, selectivity, amenability to automation and cost effectiveness [30]. The use of high performance anodic materials like lead dioxide (PbO_2) electrode can achieve high efficiency and lower the operating cost. PbO_2 has been extensively used to decompose organic contaminants owing to its high electrical conductivity, high oxygen overpotential and chemical inertness and low cost comparing with boron-doped diamond (BDD) [24,31–35]. A general scheme for the electrochemical degradation of organic compounds on metal oxide electrodes (MO_x) has been proposed [36]. H_2O is assumed to be discharged on the anode to form adsorbed hydroxyl radicals:

$$MO_x + H_2O \rightarrow MO_x(^{\bullet}OH) + H^+ + e^- \quad (1)$$

* Corresponding author. Tel.: +86 451 53625118.
E-mail address: hlliu2002@163.com (H. Liu).

0926-3373/$ – see front matter © 2008 Elsevier B.V. All rights reserved.
doi:10.1016/j.apcatb.2008.04.011

On the oxide surface, in the presence of oxidizable organic compounds (R), the following reaction takes place and the organics are decomposed by the generated hydroxyl radicals:

$$R + MO_x(^{\bullet}OH) \rightarrow CO_2 + zH^+ + MO_x + ze^- \quad (2)$$

So far, many researchers have done a large number of investigations on the electrocatalytic oxidation of *p*-NP, but few researches focus on the other two mononitrophenols (*o*-NP and *m*-NP), especially the latter. Cañizares et al. [37] proposed a simple mechanistic model for the electrochemical treatment of *p*-NP using BDD anodes. Up to now, the systematic investigations about the electrocatalytic oxidation mechanism of *o*-NP and *m*-NP have not yet been reported.

The goal of the present work was to increase our understanding of mechanism involved in the electrocatalytic oxidation of *o*-NP, *m*-NP and *p*-NP in view of the molecular configuration, including electronic character and hydrogen bond. Meanwhile, we proposed distinct degradation pathways of these NPs.

2. Experimental

O-NP, *m*-NP and *p*-NP were purchased from Aldrich and used as received. All other chemicals were analytical grade and used without further purification. Solutions were prepared using deionized *Milli-Q* water. The preparation of Bi-doped lead dioxide electrodes (Ti/Bi-PbO_2) was given in our previous work [38].

The morphology of the Bi-PbO_2 electrode was examined using a scanning electronic microscopy (SEM; USA Camscan MX2600FE). This instrument incorporated an energy dispersive X-ray analysis (EDX) for elemental analysis.

NPs concentration was measured with a LC-10A High Performance Liquid Chromatograph equipped with UV-spectrophotometer (190–360 nm). Aliquots of 10 μL were injected automatically into the HPLC to determine the concentration of NPs, using a mobile phase of methanol/water (v/v) at 70/30. The separation was performed using a Vp-ODS reversed phase column at the flow rate of 1 mL min^{-1} under 28 MPa pressure and column temperature of 303 K. Before the analysis, the mobile phase was filtered and sonicated in order to remove dissolved gas. A UV detector was used with the wavelength set at 280 nm.

Carboxylic acids were also monitored by HPLC using a HPICE-ASI DIONEX ICNPAC column with a mobile phase of 2% phosphoric acid/water at 20/60 at a flow rate of 0.8 mL min^{-1}. The UV detector was set at 210 nm.

Reaction intermediates such as hydroquinone, benzoquinone and catechol were identified by gas chromatography/mass spectrometry (GC/MS). Electron impact (EI) mass spectra were obtained with an Agilent 5976N mass spectrometer, interfaced to an Agilent 6890N gas chromatograph. The spectra were recorded by setting the electron energy to 70 eV and accelerate to 3 kV and applying a source temperature of 473 K. The magnet was scanned from 29 to 800 Da in 0.8 s. The Agilent 6890N gas chromatograph was equipped with a HP-5MS capillary column (No. 190191s-413) and FID detector. The nominal length, nominal diameter and nominal film thickness were 30 m, 0.32 mm and 0.25 μm. The auxiliary carrier gas was helium at 38.4 mL min^{-1} velocity. The oven temperature was programmed as follows: initial at 313 K for 8 min, from 313 to 593 K at 10 K min^{-1}, isothermal at 593 K for 5 min.

Nitrogen inorganic ions (NO_3^-, NO_2^-) were measured with an ion chromatograph (DIONEX 4500i) equipped with an electrical conductivity detector (ECD). Aliquots of 25 μL were injected into the IC, and carried with a mobile phase containing 1.7 mM $NaHCO_3$ and 1.8 mM Na_2CO_3. The separation was performed using a HPIC-AG4-AS4A-SC phase column at the flow rate of 1 mL min^{-1} under 780 psi. Ammonium was analyzed according to Kjeldahl method. COD was measured by a titrimetric method using dichromate as the oxidant in acidic solution at 458 K for 2 h (Hachi).

Cyclic voltammetry were tested with a standard three-electrode cell using a computer control potentiostat/galvanostat model 263A (Princeton Applied Research). Modified PbO_2 electrodes were used as working electrode, a platinum sheet as counter electrode and a saturated calomel electrode as a reference electrode. The exposed apparent area of the working electrode was 1 cm^2. The cyclic voltammetry were performed at room temperature.

The electrocatalytic oxidation experiments were carried out by batch processes and the apparatus was mainly consisted of a DC power supply, a magnetic stirrer, a water bath and a glass reactor. The anode (Ti/Bi-PbO_2) and cathode (stainless steel sheet) were positioned vertically and parallel to each other with a distance of 1 cm. All the experiments were carried out in duplicate. The initial concentration of NPs during all the experimental runs was 50 mg L^{-1} of a volume of 300 mL. The initial pH of the solution was adjusted to 4.3 ± 0.1 using 0.05 M H_2SO_4 and 0.1 M Na_2SO_4 was used as a supporting electrolyte. The reaction temperature was kept at 333 K during all the experimental runs. Electrocatalytic oxidation was performed at a current density of 30 mA cm^{-2}. The total time of electrolysis was 120 min. During the experiments, samples were drawn from the reactor at certain intervals and then analyzed.

3. Results and discussion

3.1. Cyclic voltammetry

The SEM micrograph of Ti/Bi-PbO_2 anode is shown in Fig. 1, as well as the EDX elemental analysis of this anode. Ti/Bi-PbO_2 anode has a porous structure with small-sized crystal particles and a very compact crystalline structure (Fig. 1a). The crystal size of this anode was ca. 17.491 nm in terms of our previous studies [38]. The results of EDX confirmed that Bi atoms were doped into the PbO_2 films.

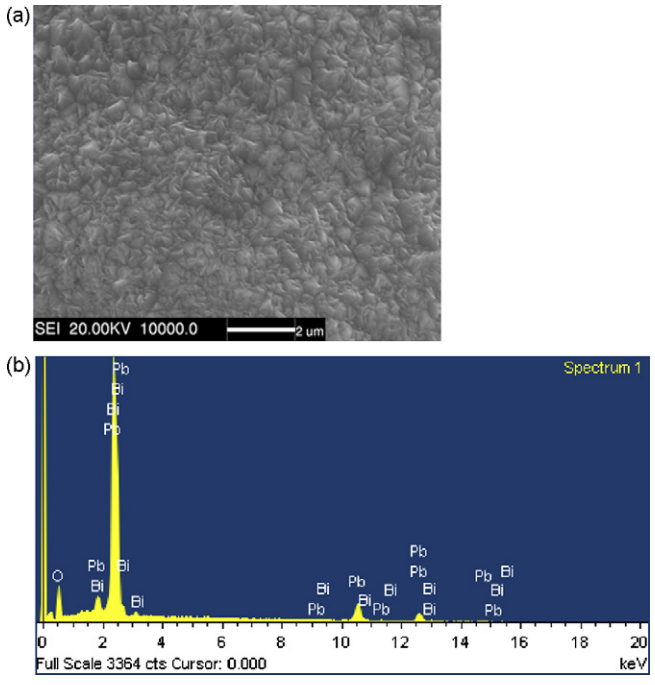

Fig. 1. SEM micrograph (a) and EDX elemental analysis (b) of Bi-PbO2 electrode.

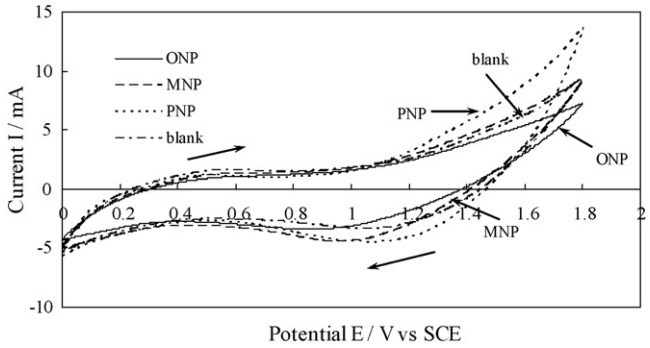

Fig. 2. Comparison of the cyclic voltammograms of different NPs at Ti/Bi-PbO_2 anodes in 0.1 M Na_2SO_4, initial NPs concentration 50 mg L^{-1}, pH 4.3, scan rate: 50 mV s^{-1}.

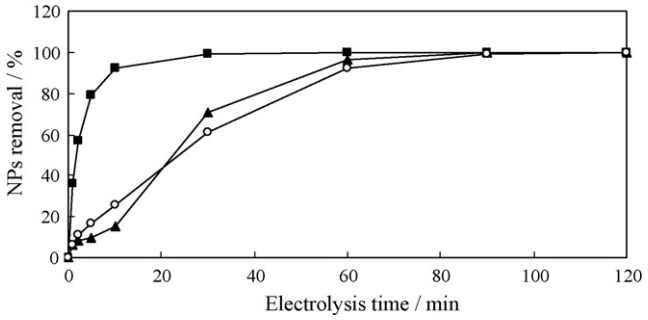

Fig. 4. Variation of NPs removal as a function of electrolysis time at Ti/Bi-PbO_2 anodes: (■) *o*-NP; (○) *m*-NP; (▲) *p*-NP, $[NPs]_0$ = 50 mg L^{-1}; pH 4.3; temperature = 333 K; current density = 30 mA cm^{-2}; $[Na_2SO_4]$ = 0.1 M.

The cyclic voltammetry curves of different NPs at Ti/Bi-PbO_2 anodes are shown in Fig. 2. Compared with the curve obtained in blank solution (without NPs), there was no new anodic current peak appeared during the positive sweeps of all the NPs. It meant that these aromatic compounds were not oxidized directly on the surface of Ti/Bi-PbO_2 anodes, but decomposed by the oxidizing agent existing in the solution, such as hydroxyl radical (•OH). Zhu et al. [27] investigated the cyclic voltammetry of *p*-NP on BDD anodes and observed an anodic current peak corresponded to the oxidation of *p*-NP. This differentiation indicates that the electrochemical behavior of Bi-doped PbO_2 is distinct from that of BDD. As we know, PbO_2 electrodes belong to 'nonactive' electrodes [39], so the organic compounds are eliminated via the interaction of ·OH that is generated by the means of the discharge of water on the surface of PbO_2 electrodes (Eq. (1)). On the other hand, other oxidants, e.g. hydrogen peroxide, peroxodisulfate ion and hypochlorite ion also play an important role in the process of organics degradation.

3.2. Electrocatalytic oxidation of NPs at Ti/Bi-PbO_2 electrode

The variation of COD removal of NPs as a function of electrolysis time is presented in Fig. 3. At the end of electrolysis, the COD removal of *o*-NP, *m*-NP and *p*-NP were 87.0%, 82.8% and 81.5%, respectively. During the first 1 h, the COD removal of *o*-NP was about 80%, while the values corresponding to *p*-NP and *m*-NP were 66.7% and 69.0%, respectively. This indicates that *o*-NP could be electrochemically oxidized more easily than *m*-NP and *p*-NP. The residual of COD indicates that some carboxylic acids formed during the degradation of NPs were not completely decomposed at the end of the electrolysis. In previous researches [25,40], the electrocatalytic oxidation of phenolic compounds would lead to the formation of carboxylic acids, which were more difficult to be decomposed than phenolic compounds. The fast removal of COD observed in the beginning could be attributed to the rapid degradation of aromatic compounds, while the final slowing down reflected a much slower mineralization of carboxylic acids originated by ring fission. The variations of COD had typical exponential shapes which illustrated that the electrocatalytic oxidation processes of NPs were mass-transfer controlled [41]. From this figure, it could also be anticipated that the COD removal would be further improved with extended electrocatalytic oxidation.

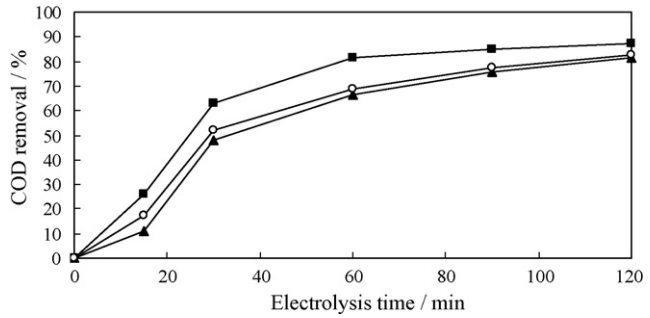

Fig. 3. Variation of COD removal as a function of electrolysis time at Ti/Bi-PbO_2 anodes: (■) *o*-NP; (○) *m*-NP; (▲) *p*-NP, $[NPs]_0$ = 50 mg L^{-1}; pH 4.3; temperature = 333 K; current density = 30 mA cm^{-2}; $[Na_2SO_4]$ = 0.1 M.

It can be seen from Fig. 4 that all the NPs were totally degraded by the 2-h electrolysis under the present experimental conditions. This figure also demonstrated a faster degradation velocity of *o*-NP, comparing with *m*-NP and *p*-NP. Previous study suggested that the degradation of some NPs was fit for pseudo-first-order kinetics [16,42]. The regression analysis of the concentration curves versus reaction time indicated that the decay of these NPs could also be described by the pseudo-first-order kinetics formula with respect to NP concentration: $dC_{NP}/dt = -kC_{NP}$. The pseudo-first-order rate constants *k* listed in Table 1 suggest that the degradation of NPs lies in the order: *o*-NP > *m*-NP > *p*-NP. The rate constant of *o*-NP was nearly twice larger than that of *p*-NP.

The Hammett constant represents the effect that the various substituents have on the electronic character of a given aromatic system [43]. A positive value indicates an electron-withdrawing group while a negative value indicates that of the electron-donating group. $-NO_2$ group is a strong electron-withdrawing substituent, so the Hammett constants are positive for all the NPs. However, the different position of the $-NO_2$ group on the aromatic ring results in different Hammett constant value. The larger the value, the stronger of electron-withdrawing capacity of the group is. The difference of rate constant may be due to the orientation of •OH radical and its subsequent reaction. The reaction of •OH radical attacking on aromatic ring is electrophilic attack. In *o*-NP, the incoming •OH radical is directly preferably to *para* position by electron-donating phenolic –OH group, while in *m*-NP and *p*-NP, the attacking to *para* position of •OH radical becomes tough owing to the steric effects of $-NO_2$ groups at the *meta* and *para* position on

Table 1
Pseudo-first-order rate constants *k* of NPs and their Hammett constants (σ) and melting point (T_{fus})

NPs	*k* (min^{-1})	Correlation coefficient R^2	σ	T_{fus} (K)
o-NP	0.0988	0.9723	1.24	318.4
m-NP	0.0709	0.9750	0.71	370.5
p-NP	0.0513	0.9157	0.78	387.3

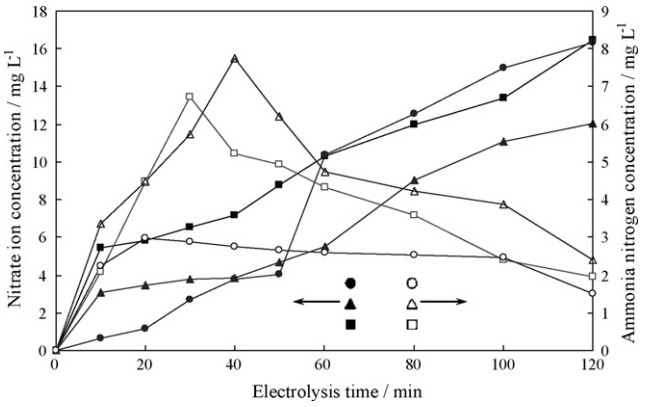

Fig. 5. Variation of nitrogen species as a function of electrolysis time of NPs at Ti/Bi-PbO_2 anodes: (■, □) *o*-NP; (●, ○) *m*-NP; (▲, □) *p*-NP.

aromatic rings, respectively. Therefore, the degradation of *o*-NP was much faster than that of *m*-NP and *p*-NP. Kavitha and Palanivelu [17] reported that the rate constants of *o*-NP were larger than those of *p*-NP in both Fenton and photo-Fenton processes. The results of researches of Chen et al. [44] indicated that the *p*-NP was more stable than *m*-NP and *o*-NP. They pointed out that the three NP isomers were the main photoproducts in the irradiated NB aqueous solutions and the yield followed the order *p*-NP > *m*-NP > *o*-NP. This meant that *p*-NP was more difficult to be decomposed by •OH radical than *m*-NP and *o*-NP, which was consistent of our investigation results.

Other than the electron-withdrawing effect of $-NO_2$ group, hydrogen bonds play an important role in the process of electrocatalytic oxidation of NPs as well. The melting point (T_{fus}) [45] listed in Table 1 follows the order: *p*-NP > *m*-NP > *o*-NP. T_{fus} is associated with the characteristics of organic compounds. As for the three NP isomers, the value of T_{fus} is concerned with the molecular structures of these compounds. There are intermolecular and intramolecular hydrogen bonds thanks to the existence of –OH group [46]. However, the different strength of these hydrogen bonds leads to the different physicochemical characteristics of NP isomers. The distinct values of T_{fus} of NP isomers reflect the different stability of these NPs. The T_{fus} is also indicates that it is much more readily to eliminate *o*-NP.

Fig. 5 shows the variation of nitrogen species as a function of electrolysis time. The formation of inorganic nitrogen species is the result of the denitration of NPs. It is worthy to mention that nitrite ions were not found in the reaction systems, which might be related to the low concentration of nitrite ions led by their short lifetime in the solution. The formation of ammonia indicated the reduction of NPs took place at the cathode. Cañizares et al. [37] and Nasr and Abdellatif [41] also confirmed the generation of ammonia in the process of electrocatalytic oxidation of *p*-NP and 2,4,6-trinitrophenol using BDD as anodes, respectively. This species was also oxidized and transformed to nitrate at the end of electrolysis. The initial concentration of organic nitrogen in the NPs reaction system was 0.36 mM, and the total inorganic nitrogen concentrations of *o*-NP, *m*-NP and *p*-NP were 0.353, 0.346 and 0.327 mM, respectively, at the end of reaction. The mass balance results for nitrogen revealed that the

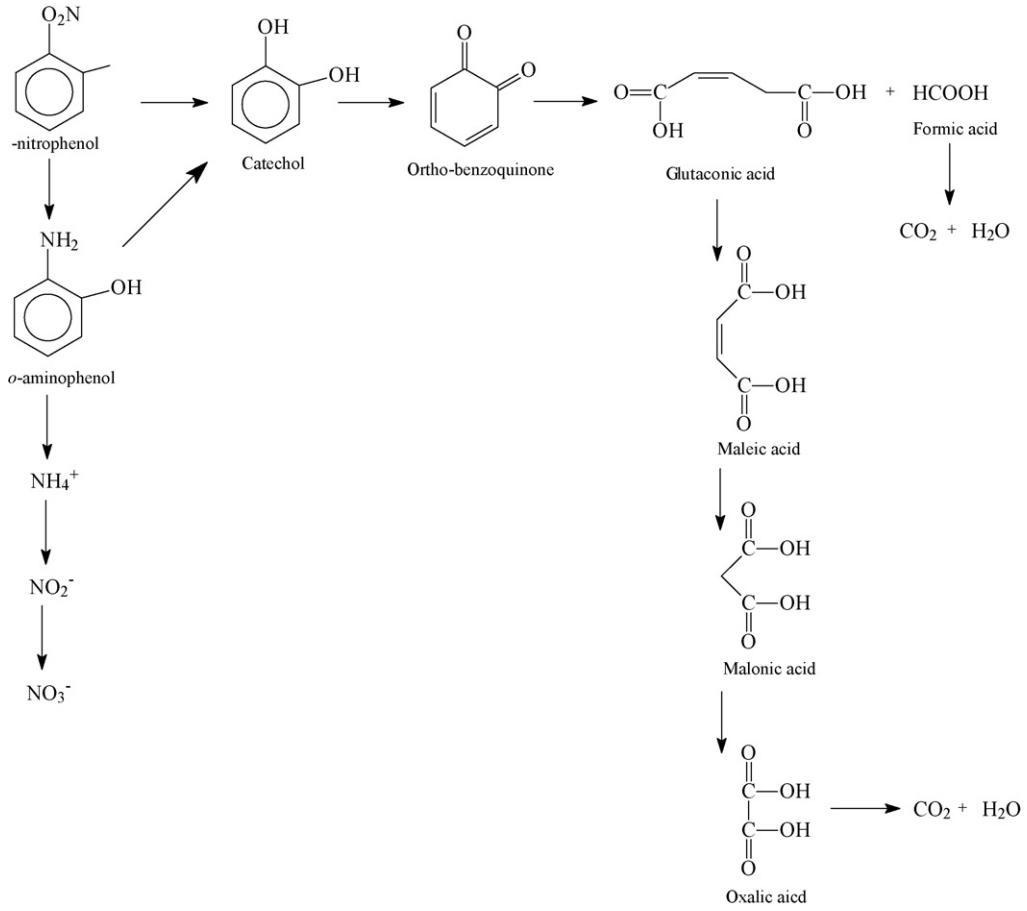

Fig. 6. Possible degradation pathway of *o*-NP at Ti/Bi-PbO_2 anodes.

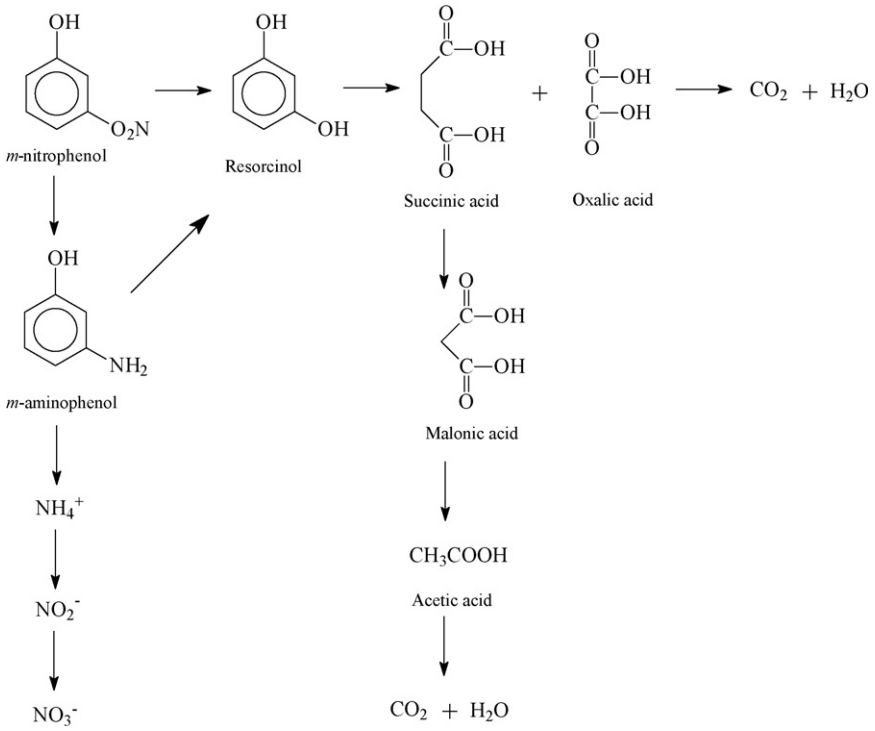

Fig. 7. Possible degradation pathway of *m*-NP at Ti/Bi-PbO_2 anodes.

$-NO_2$ groups of both *o*-NP and *m*-NP were almost completely removed from the aromatic ring.

3.3. Proposed mechanism of electrocatalytic oxidation of NPs

Based on the above findings, a tentative reaction pathway for mineralization of *o*-NP, *m*-NP and *p*-NP to CO_2 at present experimental conditions are presented in Figs. 6–8, respectively. GC/MS and HPLC were used to monitor the intermediates and carboxylic acids generated during the oxidation processes.

·OH radical has a strong electrophilic character, and $-NO_2$ group is a strong electron-withdrawing substituent. Therefore, $-NO_2$ group was attacked by •OH radical causing them to become detached from the aromatic ring, at the first stage of oxidation [17,37]. Catechol, resorcinol and hydroquinone detected by GC/MS clarified the above speculation. At the meantime, GC/MS found the

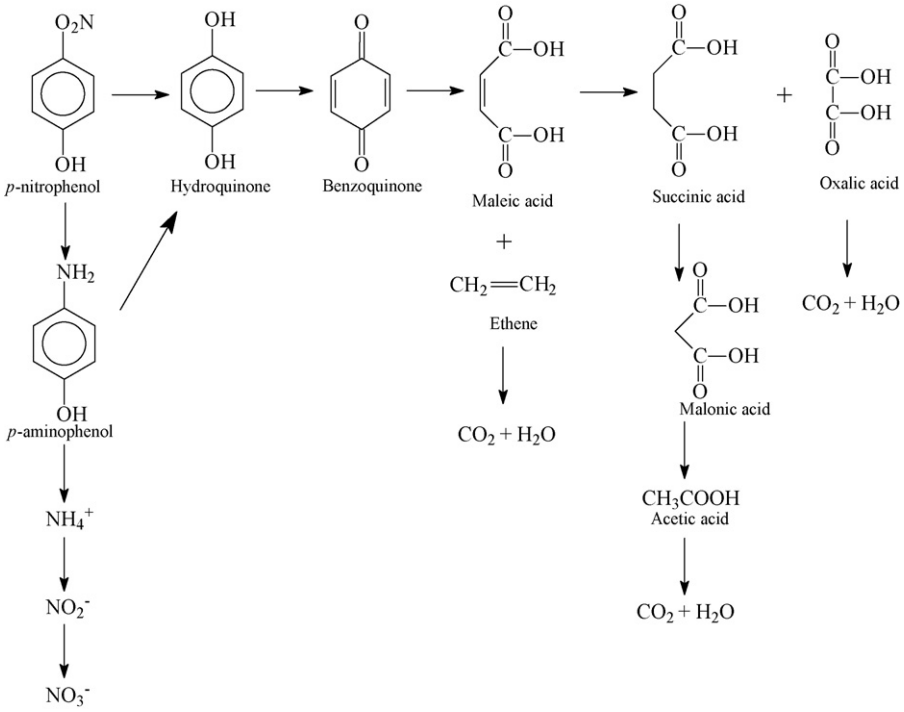

Fig. 8. Possible degradation pathway of *p*-NP at Ti/Bi-PbO_2 anodes.

existence of aminophenols (APs) as well. This phenomenon indicated that the reduction of NPs to APs took place at the cathode. Then, these APs disappeared gradually with the electrolysis went on. Previous researches [23,37] reported that APs would be polymerized to transform into a dark brown solid that remained on the surface of cathode up to the end of treatment. However, this dark brown solid was not observed in all of our experimental runs. It can be inferred that these APs were completely oxidized ultimately. Subsequently, *ortho*-benzoquinone and benzoquinone were detected in the electrolytes of *o*-NP and *p*-NP, respectively. The change of the color of the two electrolytes also confirmed the generation of quinonic compounds. In the initial period of the present experiment, the electrolyte color of *o*-NP and *p*-NP turned to light yellow. Then, the color became darker after a period of time and finally became colorless again. As for *m*-NP, no quinonic was detected and the color of the electrolyte faded gradually and finally became colorless. In turn, these quinonic compounds and resorcinol were subjected to further attack by $^{\bullet}OH$ radical, eventually leading to aromatic ring opening and the formation of a series of carboxylic acids. Glutaconic acid, maleic acid and oxalic acid were the main aromatic ring opening products detected by HPLC. And some small amount of succinic acid, malonic acid and acetic acid were also monitored. The compositions of the carboxylic acids were different in the different electrolytes of NPs. Finally, these carboxylic acids were oxidized into CO_2 and H_2O. The detailed reaction pathways of three NPs isomers were presented in Figs. 6–8, respectively.

4. Conclusions

The following conclusions can be drawn from the present experiments:

1. Electrocatalytic oxidation using Bi-doped lead dioxide anode can be successfully used for the treatment of aqueous NPs wastes. The total removal of the organic compounds is achieved under the chosen experimental conditions.
2. The uncompleted COD removal confirms the carboxylic acids are more difficult to be decomposed than NPs. The profiles of COD variation illustrate that the electrocatalytic oxidation processes of NPs are mass-transfer controlled.
3. The electrocatalytic oxidation processes of NPs can be modeled as a pseudo-first-order. The value of the pseudo-first-order rate constants of the three isomers demonstrates the oxidation of them lies in the order: *o*-NP > *m*-NP > *p*-NP. The electron character and hydrogen bonds significantly influence the electrocatalytic oxidation of NPs.
4. Nitrate ion is identified as the major nitrogen final reaction product during the NPs oxidation, while a minor amount of ammonia is left at the end of electrolysis.
5. The main intermediates of the oxidation of NPs are hydroquinone, catechol, resorcinol, benzoquinone, aminophenols, glutaconic acid, maleic acid and oxalic acid.
6. The possible degradation pathways of NPs are proposed. According to these models, the first stage is the release of nitro group from the aromatic rings. As a consequence, hydroquinone, catechol, resorcinol and benzoquinone are formed. These organic compounds are oxidized first to carboxylic acids (glutaconic acid, maleic acid and oxalic acid) and later to carbon dioxide and water. Simultaneously, the reduction of NPs to aminophenols takes place at the cathode. But these aminophenols are all oxidized to carbon dioxide and water eventually.

Acknowledgements

This work was supported by Program for Changjiang Scholars and Innovative Research Team in University (PCSIRT), the Ministry of Education, China.

References

[1] M. Shimazu, A. Mulchandani, W. Chen, Biotechnol. Bioeng. 76 (2001) 318–324.
[2] J.B. Lippincot, List of Worldwide Hazardous Chemical and Pollutants, The Forum for Scientific Excellence, New York, 1990.
[3] M.S. Dieckmann, K.A. Gray, Water Res. 30 (1996) 1169–1183.
[4] J. Kiwi, C. Pulgarin, C. Peringer, Appl. Catal. B: Environ. 3 (1994) 335–350.
[5] A. Gutes, F. Cespedes, S. Alegret, M. Del Valle, Biosens. Bioelectron. 20 (2005) 1668–1673.
[6] USEPA, Health and environmental effects profile for nitrophenols [S], Environmental Protection Agency, Environmental Criteria and Assessment Office, Cicinnati, OH: US, 1985.
[7] ATSDR (Agency for Toxic Substance and Disease Registry) Toxicological Profile for NPs, Department of Health and Human Service, Public Health Service, Atlanta, GA, US, 1992.
[8] USEPA, Nitrophenols: Ambient Water Quality Criteria, Washington, DC, 1980.
[9] S. Yi, W.Q. Zhuang, B. Wu, S.T.L. Tay, J.H. Tay, Environ. Sci. Technol. 40 (2006) 2396–2401.
[10] M.C. Tomei, M.C. Annesini, Environ. Sci. Technol. 39 (2005) 5059–5065.
[11] Z.I. Bhatti, H. Toda, K. Furukawa, Water Res. 36 (2002) 1135–1142.
[12] M.C. Tomei, M.C. Annesini, R. Luberti, G. Cento, A. Senia, Water Res. 37 (2003) 3803–3814.
[13] Y. Lee, J. Yoon, U. Von Gunten, Environ. Sci. Technol. 39 (2005) 8978–8984.
[14] M. Sivakumar, P.A. Tatake, A.B. Pandit, Chem. Eng. 85 (2002) 327–338.
[15] Q.L. Lu, G.A. Sorial, J. Hazard. Mater. 148 (2007) 436–445.
[16] A. Goi, M. Trapido, Chemosphere 46 (2002) 913–922.
[17] V. Kavitha, K. Palanivelu, J. Photochem. Photobiol. A Chem. 170 (2005) 83–95.
[18] M.A. Oturan, J. Perioten, P. Chartrin, A.J. Acher, Environ. Sci. Technol. 34 (2004) 3474–3479.
[19] S.H. Yuan, M. Tian, Y.P. Cui, L. Lin, X.H. Lu, J. Hazard. Mater. B 137 (2006) 573–580.
[20] M.H. Priya, G. Madras, Ind. Eng. Chem. Res. 45 (2006) 482–486.
[21] T.A. Egerton, P.A. Christensen, R.W. Harrison, J.W. Wang, J. Appl. Electrochem. 35 (2005) 799–813.
[22] M.E. Suarez-Ojeda, F. Stuber, A. Fortuny, A. Fabregat, J. Carrera, J. Font, Appl. Catal. B: Environ. 58 (2005) 105–114.
[23] L. Oliviero, J. Barbier, D. Duprez, Appl. Catal. B: Environ. 40 (2003) 163–184.
[24] M.A. Quiroz, S. Reyna, C.A. Martínez-Huitle, S. Ferro, A. De Battisti, Appl. Catal. B: Environ. 59 (2005) 259–266.
[25] P. Cañizares, J. Lobato, R. Paz, M.A. Rodrigo, C. Sáez, Water Res. 39 (2005) 2687–2703.
[26] C. Borrás, C. Berzoy, J. Mostany, J.C. Herrera, B.R. Scharifker, Appl. Catal. B: Environ. 72 (2007) 98–104.
[27] X.P. Zhu, S.Y. Shi, J.J. Wei, F.X. Lv, H.Z. Zhao, J.T. Kong, Q. He, J.R. Ni, Environ. Sci. Technol. 41 (2007) 6541–6546.
[28] C. Borrás, T. Laredo, J. Mostany, B.R. Scharifker, Electrochim. Acta 49 (2004) 641–648.
[29] M.H. Zhou, L.C. Lei, Chemosphere 65 (2006) 1197–1203.
[30] K. Rajeshwar, J.G. Ibanez, Environmental Eelectrochemistry: Fundamentals and Aapplications in Pollution Abatement, Academic Press, San Diego, CA, 1997.
[31] J. Feng, D.C. Johnson, J. Electrochem. Soc. 138 (1991) 3329–3337.
[32] M. Panizza, G. Cerisola, Appl. Catal. B: Environ. 75 (2007) 95–101.
[33] M.H. Zhou, Z.C. Wu, X.J. Ma, Y.Q. Cong, Q. Ye, D.H. Wang, Sep. Sci. Technol. 34 (2004) 81–88.
[34] D.C. Johnson, J. Feng, L.L. Houk, Electrochim. Acta 46 (2000) 323–330.
[35] M.H. Zhou, Q.Z. Dai, L.C. Lei, C.A. Ma, D.H. Wang, Environ. Sci. Technol. 39 (2005) 363–370.
[36] Ch. Comninellis, Electrochim. Acta 39 (1994) 1857–1862.
[37] P. Cañizares, C. Sáez, J. Lobato, M.A. Rodrigo, Ind. Eng. Chem. Res. 43 (2004) 1944–1951.
[38] H.L. Liu, Y. Liu, C. Zhang, R.S. Shen, J. Appl. Electrochem. 38 (2008) 101–108.
[39] P. Cañizares, F. Martínez, M. Díaz, J. García-Gómez, M.A. Rodrigo, J. Electrochem. Soc. 149 (2002) D118–D124.
[40] B. Nasr, G. Abdellatif, P. Cañizares, C. Sáez, M.A. Rodrigo, Environ. Sci. Technol. 39 (2005) 7234–7239.
[41] B. Nasr, G. Abdellatif, J. Appl. Electrochem. 152 (2005) D113–D116.
[42] S.Y. Ai, M.N. Gao, W. Zhang, Q.J. Wang, Talanta 62 (2004) 445–450.
[43] J.A. Dean, Handbook of Organic Chemistry, McGraw-Hill, New York, 1987.
[44] B. Chen, C. Yang, N.K. Goh, J. Environ. Sci. 17 (2005) 886–893.
[45] A. Heintz, S. Kapteina, S.P. Verevkin, J. Phys. Chem. A 111 (2007) 6552–6562.
[46] M. Shamsipur, M.R. Fat'hi, Y. Yamini, A.R. Ghiasvand, J. Supercrit. Fluids 23 (2002) 225–231.